

Zonally asymmetric temperature structure around the tropical tropopause and its relationship to deep convection

Eriko Nishimoto and Masato Shiotani

Research Institute for Sustainable Humanosphere (RISH), Kyoto University, Japan.

eriko@rish.kyoto-u.ac.jp

1. Introduction

The tropical tropopause temperature is primarily important to dehydrate air entering the lower stratosphere. It is known that there exists a "horseshoe-shaped" temperature structure in the solstice seasons. Some numerical studies [e.g., Highwood and Hoskins, 1998] showed that it is stationary wave response of the Matsuno-Gill pattern (Fig. 1).

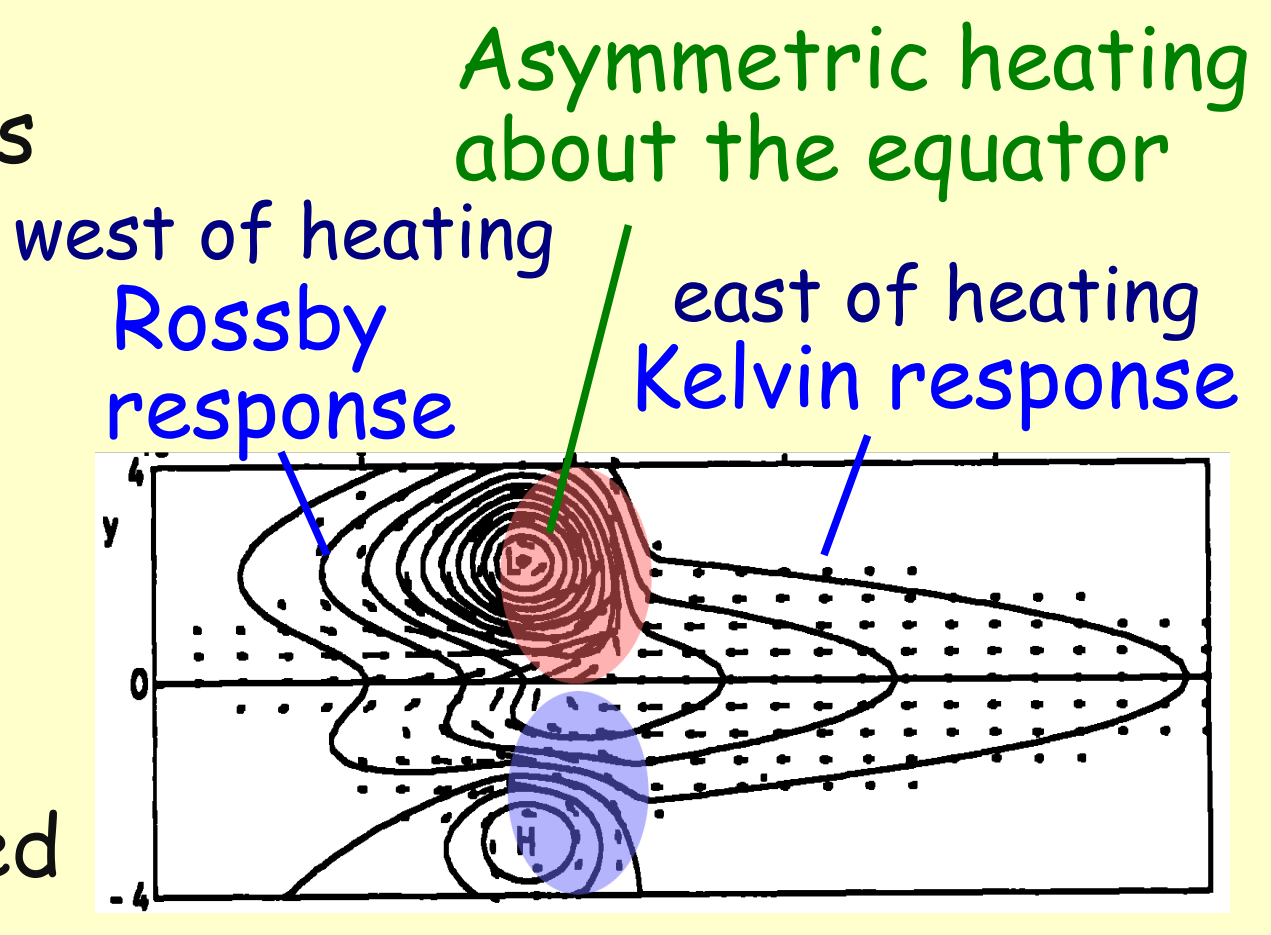


Fig. 1: Matsuno-Gill pattern (adapted from Gill [1980])

Studying variability of the tropopause temperature is important to assess a process of the stratosphere-troposphere exchange. In this study, we survey spatial and temporal variability of the horseshoe-shaped temperature structure using the reanalysis data.

2. Data

- We use the following data for about 23 years from Jan 1979 to Aug 2002.
- ERA-40 Temperature @ 100hPa
- Outgoing Longwave Radiation (OLR) as a proxy of deep convection
- Southern Oscillation Index (SOI) to assess the ENSO effect

3. Climatological Horseshoe-shaped Structure

It is conspicuous that horseshoe-shaped temperature structures exist in the solstice seasons; cold anomaly on the equator extends to north-west and south-west (Fig. 2). It looks like the Matsuno-Gill pattern with asymmetric heating on the equator (Fig. 1).

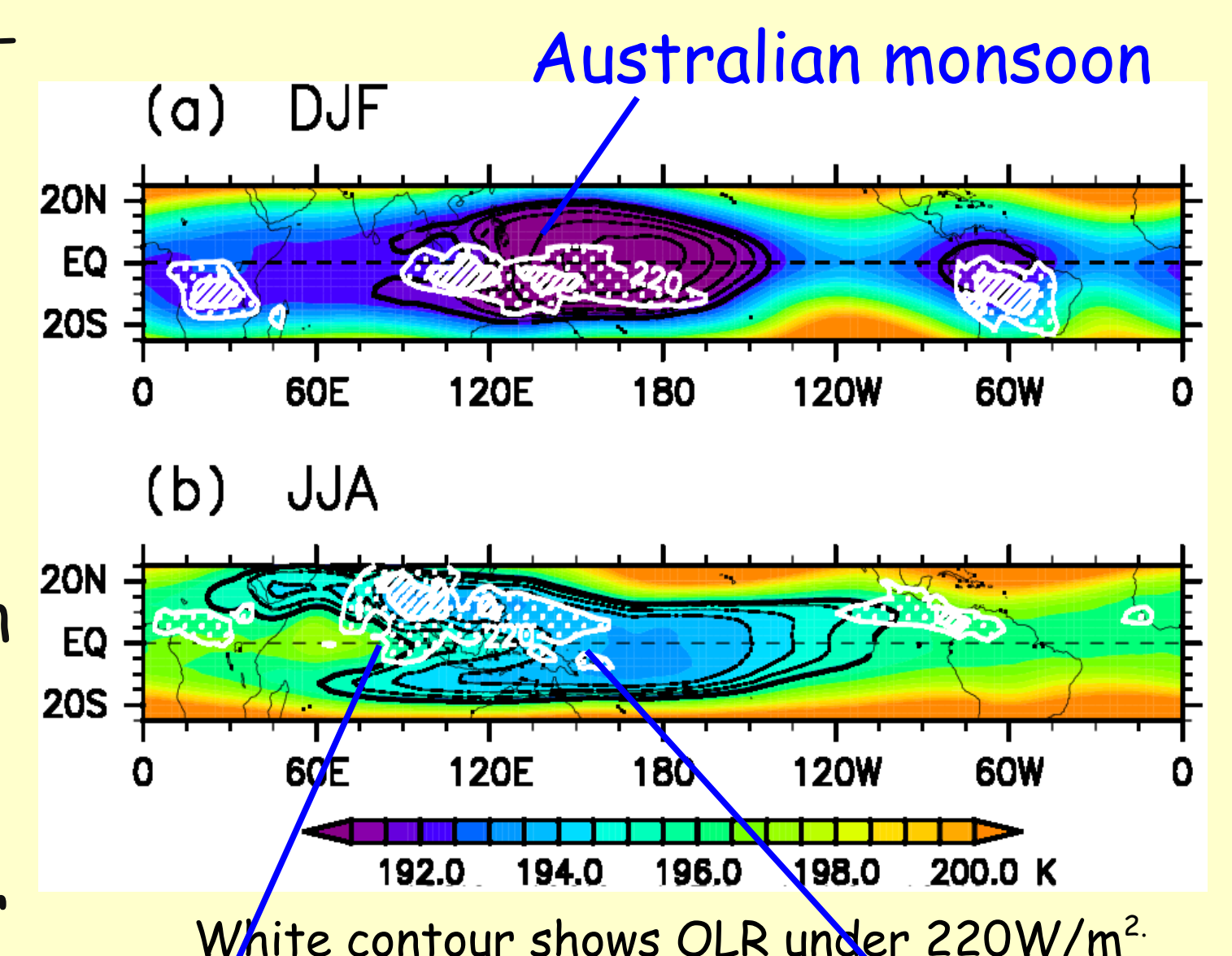


Fig. 2: Maps of temperature (K) at 100hPa and OLR (W/m²) averaged over 23 years during (a) Dec-Feb and (b) Jun-Aug.

We found two convection areas that are far away from the equator in these seasons. One is the Australian monsoon region during Dec-Feb. The other is the Asian monsoon region, which is divided into two regions (SEAM and WNPM) during Jun-Aug.

4. Definition of Indices

Paying attention to the horseshoe-shaped cold anomaly, we define two indices as follows:

- HSIy** (the latitudinal component of HorseShoe Index)
- HSIx** (the longitudinal component of HorseShoe Index)

$$HSIy = \frac{T(10^{\circ}N \sim 15^{\circ}N) + T(10^{\circ}S \sim 15^{\circ}S)}{2} - T_{eq}$$

$$HSIx(\lambda) = T_{eq}(\lambda + 10^{\circ}) - T_{eq}(\lambda - 10^{\circ})$$

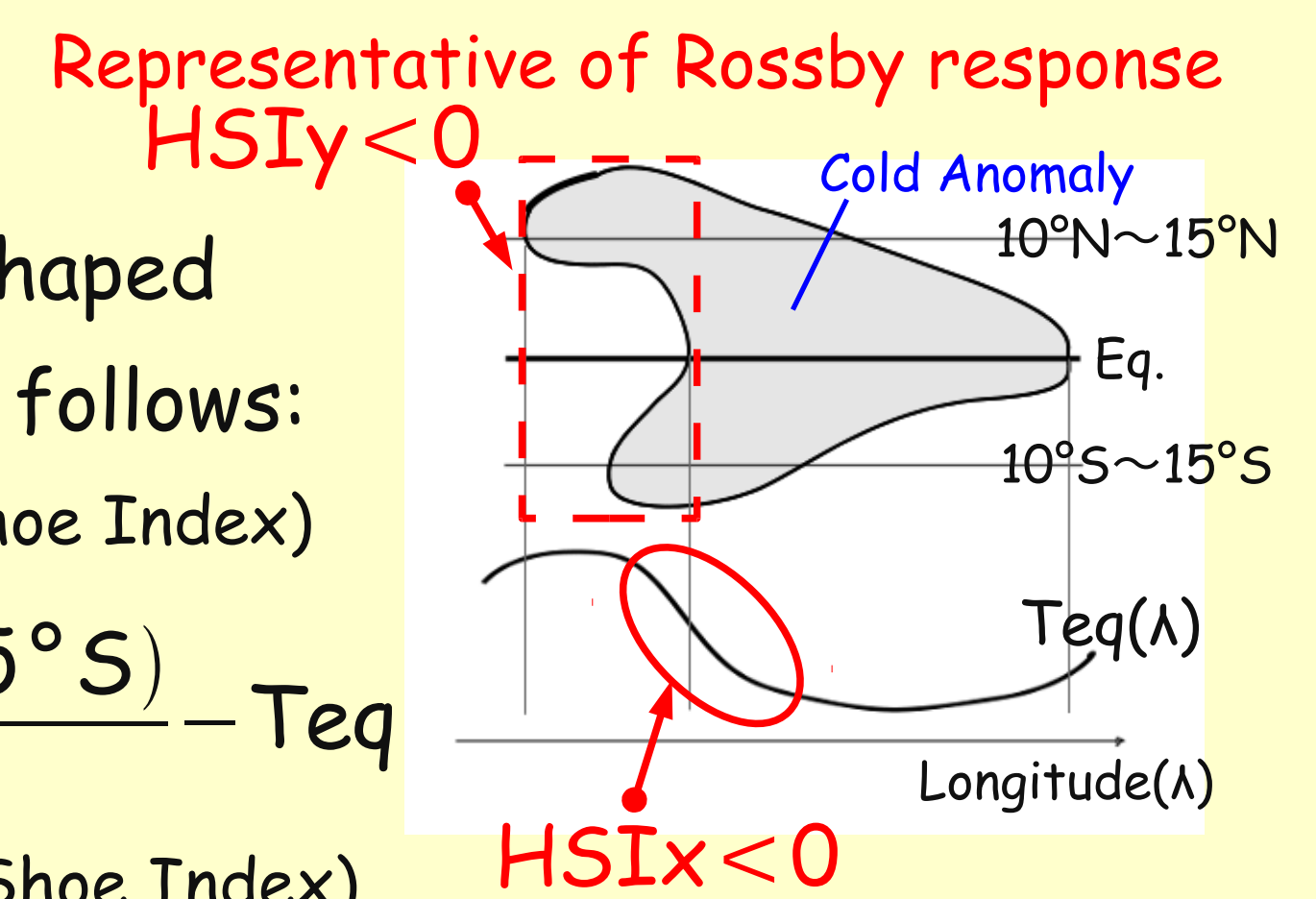


Fig. 3: Diagram showing an explanation of the indices.

5. Seasonality Corresponding to Monsoon Regions

We show longitude-time sections of HSIy in Fig. 4, HSIx in Fig. 5 and tropical mean convective activity in Fig. 6. They are averaged over 23 years. We found distinct seasonal variations in the Eastern Hemisphere; there are peaks of negative HSIy, negative HSIx, and convective activity during the southern and northern summer. The negative HSIy is located in the west of the convection area, and the negative HSIx in the east of it. These positions are consistent with those of Rossby and Kelvin responses with respect to a heating position in the Matsuno-Gill pattern.

The convection areas are related to the Australian monsoon (southern summer) and the Asian monsoon (northern summer; SEAM and WNPM) regions. SEAM and WNPM regions are distinctly separated at 120°E. The seasonality between the negative HSIx and the convective activity is in a good correspondence. In different to them, the negative HSIy during the northern summer is much clear and extended wider than during the southern summer. This seasonality almost agrees with that of Dunkerton [1995], who found that anticyclones adjacent to the Asian monsoon region and, to a lesser extent, the Australian monsoon region, are remarkable around the tropopause.

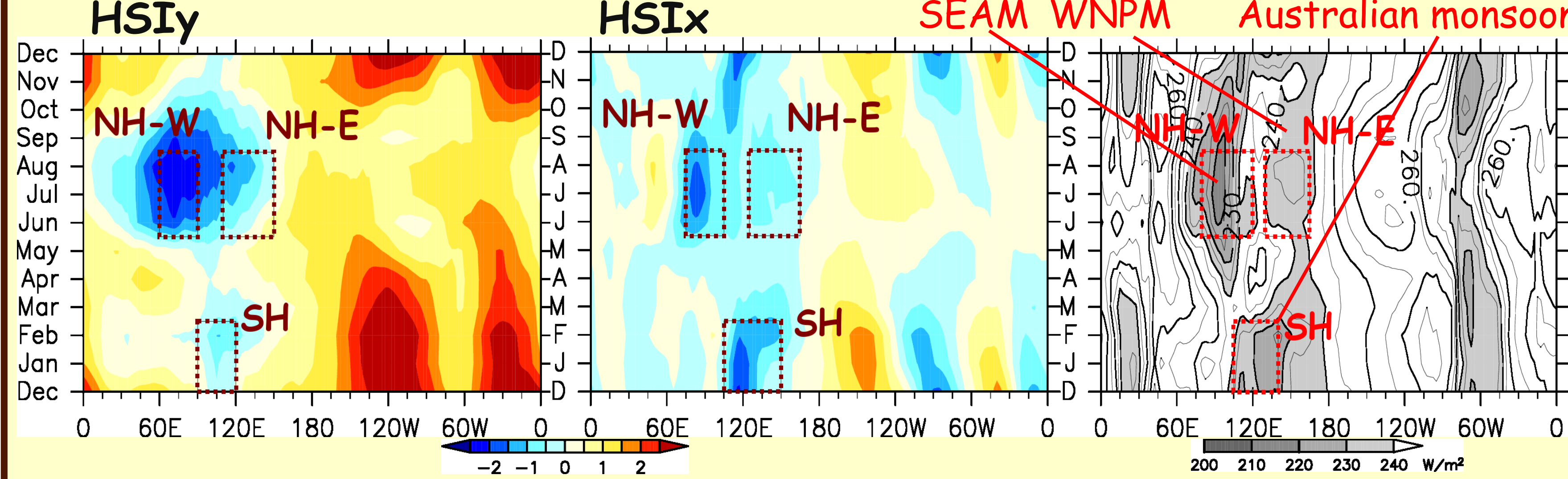


Fig. 4 (left) Longitude-time sections of HSIy, Fig. 5 (middle) of HSIx and Fig. 6 (right) of tropical (20°S-20°N) mean OLR. They are averaged over 23 years.

6. Linear Response to Variations in Monsoon Regions

Here, we average the indices over the three regions (SH, NH-W, NH-E), where the negative peaks of HSIy and HSIx are located. They are denoted in Figs. 4, 5 and 6. Note that OLR in SH (NH-W, NH-E) are averaged over the region between 15°S and 5°N (5°S and 15°N), which corresponds to the convection area in Fig. 2.

We expect that the Rossby and Kelvin wave responses to changes in heating intensity are correlated in a linear regression. This idea is supported by clear relationships between HSIy and HSIx with large variances in SH (Fig. 7-a), and significant correlations in NH-W (Fig. 7-b) and NH-E (Fig. 7-c).

Links to convective activities are also observed in SH (Fig. 8-a) and NH-E (Fig. 8-c); their variances are large, particularly in SH, but, the correlation coefficient in NH-W (Fig. 8-b) is not high.

In NH-E, during Jun to Aug, the convective activity is gradually intensified; this results in an enhancement of the anomaly (Figs. 7-c and 8-c).

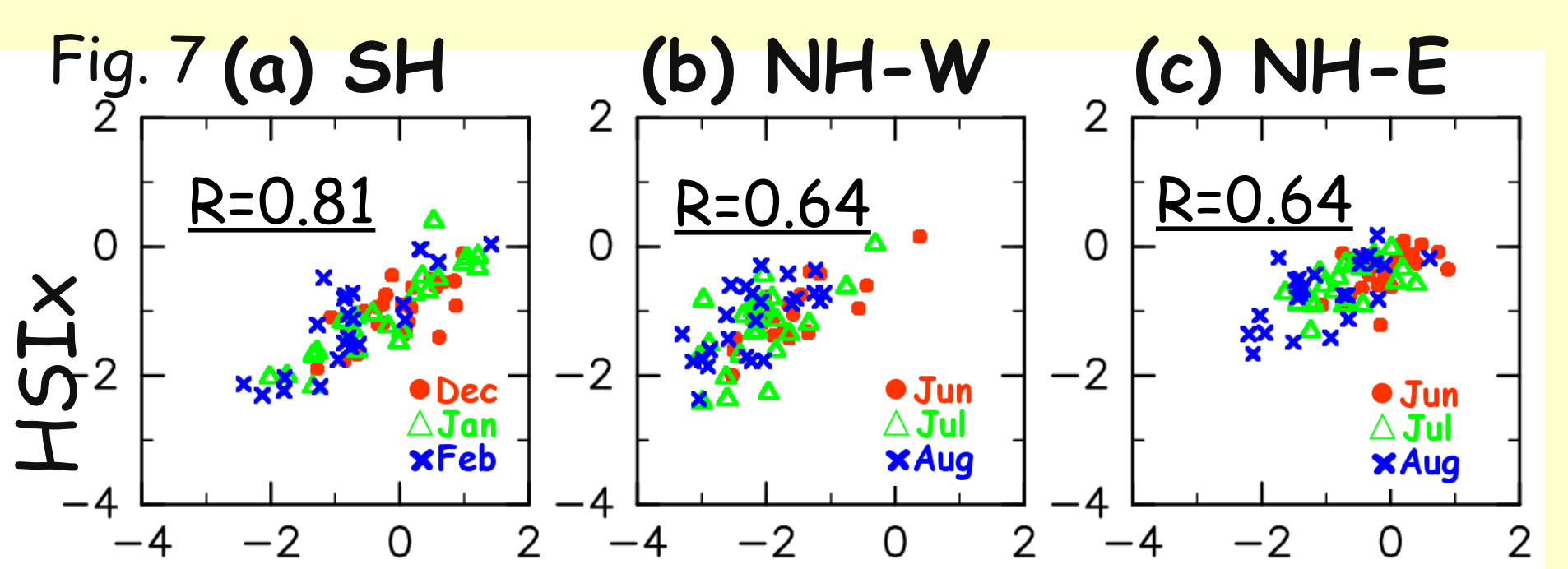


Fig. 7 (top) Scatter plots of HSIy versus HSIx, Fig. 8 (bottom) OLR versus HSIy. They are monthly mean value, and averaged over the region of (a) SH, (b) NH-W and (c) NH-E.

7. Interannual Variability and its Link to ENSO

In the tropical region, the ENSO cycle is a dominant interannual variation that involves migrations of convection areas. We surveyed interannual variability of horseshoe-shaped cold anomalies (Figs.9 and 10) and effects of ENSO on them (Table 1). Moreover, Fig. 11 shows variations of the tropopause temperature and convection areas; the variations are affected by the ENSO cycle.

During the southern summer, when an impact of ENSO is strong (Fig. 11-a), the ENSO cycle produces large variations of the horseshoe-shaped cold anomaly (Figs. 9-a and 10-a, and Table 1). These variations may result from a migration of convective activity over the Western Pacific (Fig. 11-a).

During the northern summer, there are small interannual variations of the horseshoe-shaped cold anomalies (Figs. 9-b and 9-c); however, there is no relation to convective activity in NH-W (Fig. 10-b). A migration of convective activity, which is located outside NH-W, over the Western Pacific (Fig. 11-b) may produce the variation in NH-W. We find no evidence of links to the ENSO cycle in NH-E (Table 1).

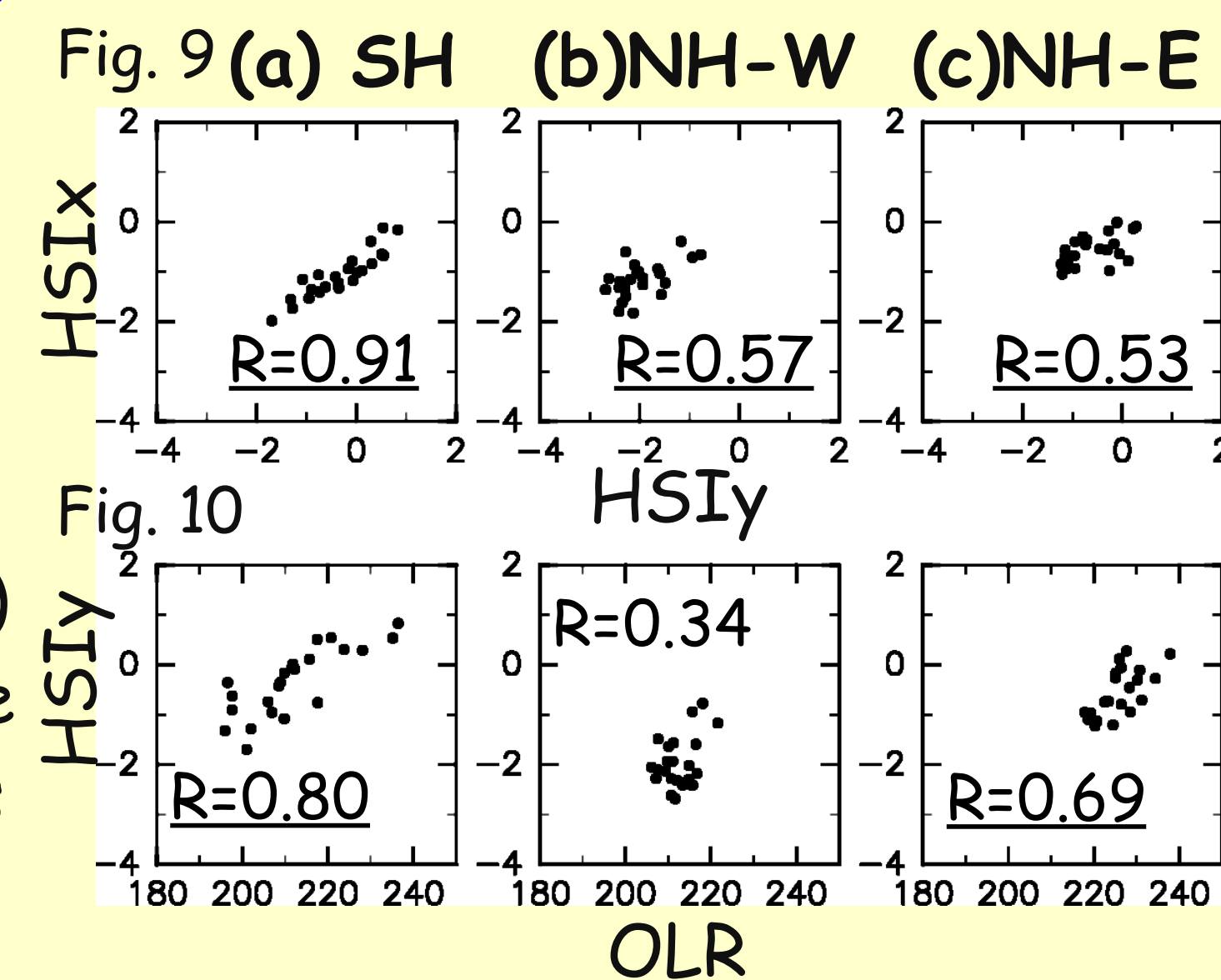


Fig. 9 (top) Scatter plots of 3-month mean HSIy versus HSIx, Fig. 10 (bottom) OLR versus HSIy, which are averaged over the region of (a) SH, (b) NH-W and (c) NH-E.

Table 1: Correlation coefficient between SOI and HSIy, HSIx, OLR.

	SH	NH-W	NH-E
SOI-HSIy	-0.61	-0.61	-0.04
SOI-HSIx	-0.75	-0.59	0.03
SOI-OLR	-0.91	-0.48	0.15

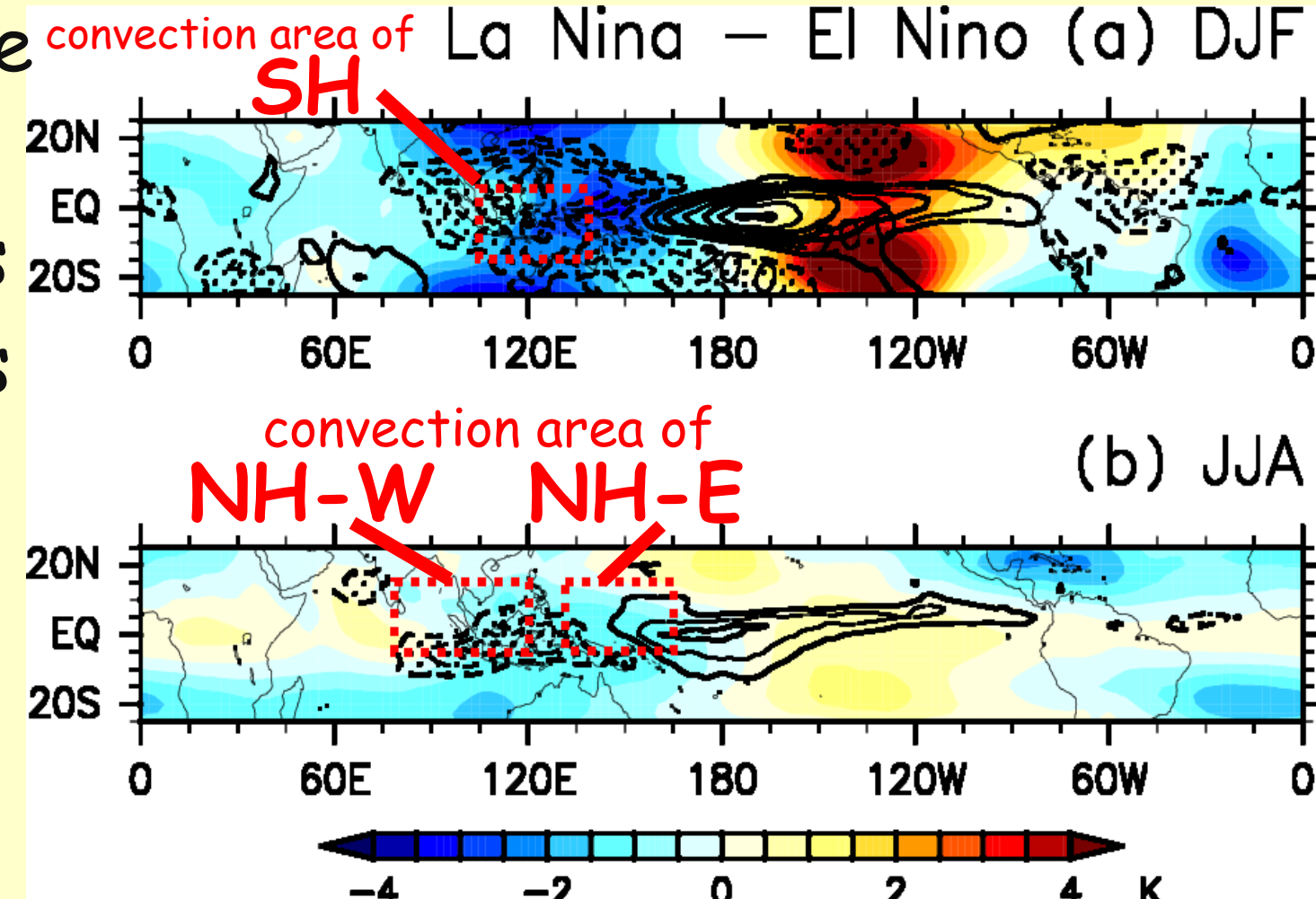


Fig. 11: Composite differences (La Niña minus El Niño) of the temperature at 100hPa (color) and OLR (contour) during (a) Dec-Feb and (b) Jun-Aug.

8. Summary

Variability of a horseshoe-shaped cold anomaly around the tropical tropopause has been investigated. Its seasonality and locality show a good correspondence to monsoon convection. During the southern summer, we found a clear relation of the cold anomaly to the Australian monsoon and ENSO. During the northern summer, there are two active monsoon regions over the Indian Ocean and the Western Pacific. The extended cold anomalies show different variability in each other.

Refs. Dunkerton, T. J. (1995), J. Geophys. Res., 100, 16675-16688.
 Gill, A. E. (1980), Q. J. R. Meteorol. Soc., 106, 447-462.
 Highwood, E. J. and B. J. Hoskins (1998), Q. J. R. Meteorol. Soc., 124, 1579-1604.
 Murakami, T. and J. Matsumoto (1994), J. Meteor. Soc. Jpn., 72(5), 719-745.